



## A CVD diamond detector for (n, $\alpha$ ) cross-section measurements

---

**C. Weiss<sup>\*1,2</sup>, G. Badurek<sup>1</sup>, E. Berthoumieux<sup>3</sup>, M. Calviani<sup>2</sup>, E. Chiaveri<sup>3</sup>, D. Dobos<sup>2</sup>, E. Griesmayer<sup>1</sup>, C. Guerrero<sup>2</sup>, E. Jericha<sup>1</sup>, F. Käppeler<sup>4</sup>, H. Leeb<sup>1</sup>, T. Rauscher<sup>5</sup> and V. Vlachoudis<sup>2</sup>**

<sup>1</sup> *Vienna University of Technology*

*Vienna, Austria*

<sup>2</sup> *CERN*

*Geneva, Switzerland*

<sup>3</sup> *CEA Saclay*

*IRFU, F-91191 Gif-sur-Yvette, France*

<sup>4</sup> *Karlsruhe Institute of Technology, Campus Nord*

*Karlsruhe, Germany*

<sup>5</sup> *University of Basel*

*Basel, Switzerland*

*E-mail:* [christina.weiss@cern.ch](mailto:christina.weiss@cern.ch), [badurek@ati.ac.at](mailto:badurek@ati.ac.at),  
[eric.berthoumieux@cern.ch](mailto:eric.berthoumieux@cern.ch), [marco.calviani@cern.ch](mailto:marco.calviani@cern.ch),  
[enrico.chiaveri@cern.ch](mailto:enrico.chiaveri@cern.ch), [daniel.dobos@cern.ch](mailto:daniel.dobos@cern.ch),  
[erich.griesmayer@cern.ch](mailto:erich.griesmayer@cern.ch), [carlos.guerrero@cern.ch](mailto:carlos.guerrero@cern.ch),  
[jericha@ati.ac.at](mailto:jericha@ati.ac.at), [franz.kaeppler@kit.edu](mailto:franz.kaeppler@kit.edu), [leeb@ati.ac.at](mailto:leeb@ati.ac.at),  
[thomas.rauscher@unibas.ch](mailto:thomas.rauscher@unibas.ch), [vasilis.vlachoudis@cern.ch](mailto:vasilis.vlachoudis@cern.ch)

In astrophysics, the determination of the optical  $\alpha$ -nucleus potential for low  $\alpha$ -particle energies, crucial in understanding the origin of the stable isotopes, has turned out to be a challenge. Theory still cannot predict the optical potentials required for the calculation of the astrophysical reaction rates in the Hauser-Feshbach statistical model and there is scant experimental information on reactions with  $\alpha$  particles at the relevant astrophysical energies. Measurements of (n,  $\alpha$ ) cross-sections offer a good opportunity to study the  $\alpha$  channel.

At the n\_TOF experiment at CERN, a prototype detector, based on the chemical vapor deposition (CVD) diamond technology, has been recently developed for (n,  $\alpha$ ) measurements. A reference measurement of the  $^{10}\text{B}(n, \alpha)^7\text{Li}$  reaction was performed in 2011 at n\_TOF as a feasibility study for this detector type.

The results of this measurement and an outline for future experiments are presented here.

*VI European Summer School on Experimental Nuclear Astrophysics, ENAS 6  
September 18-27, 2011  
Acireale Italy*

---

\*Speaker.

## 1. Introduction

At the neutron time-of-flight facility (n\_TOF) at CERN [1] the cross-sections of neutron-induced nuclear reactions are measured over a wide neutron energy ( $E_n$ ) range. For the investigation of (n,  $\alpha$ ) reactions, a prototype detector, based on the chemical vapor deposition (CVD) diamond technology, was developed and tested in the neutron beam in 2011.

The experimental observable in the measurement of the neutron cross-section of a given reaction is the reaction yield  $Y(E_n)$ . For the (n,  $\alpha$ ) reaction it is given by:

$$Y_\alpha(E_n) = \left(1 - e^{-n\sigma_t(E_n)}\right) \frac{\sigma_\alpha(E_n)}{\sigma_t(E_n)}, \quad (1.1)$$

where  $\sigma_t(E_n)$  and  $\sigma_\alpha(E_n)$  are the total and the (n,  $\alpha$ ) cross-sections of the isotope under investigation, respectively. The number of atoms per projected area of this isotope is given by  $n$ . The reaction yield can be experimentally obtained by:

$$Y_\alpha(E_n) = \frac{C(E_n) - B(E_n)}{\varepsilon_\alpha(E_n) \cdot \Phi_n(E_n) \cdot BIF}. \quad (1.2)$$

Here  $C(E_n)$  are recorded counts during the measurement of the sample and  $B(E_n)$  are background events.  $\Phi_n(E_n)$  is the neutron fluence at the experiment,  $BIF$  the beam interception factor for the experiment and  $\varepsilon_\alpha(E_n)$  is the efficiency of the experimental setup.

The aim of this measurement was to identify  $\varepsilon_\alpha(E_n)$  of the prototype detector, its response to the neutron beam and possible aspects that need to be improved in future applications of CVD diamond detectors for cross-section measurements.

## 2. CVD diamond as detector material

Diamond is a semi-conducting material with a band gap of 5.5 eV, which makes it

a very low-noise and light-insensitive detector material. The ionization energy of 13.6 eV results in a comparably low charge yield. In combination, diamond is a suitable material even for single minimum ionizing particle (MIP) detection [2]. The mobility of the charge carriers is 1700 and 2100 cm<sup>2</sup>/Vs for electrons (e<sup>-</sup>) and holes (h), respectively [3]. This makes diamond a detector material with a very fast response and a particle discrimination capability in the nano-second range. Diamond has a displacement threshold energy of 43 eV/atom. It is a radiation-hard material, suited for applications in accelerator environments.

CVD diamonds are grown in plasma reactors on a suitable seed. To date, commercially available detector-grade CVD diamond materials are single-crystal (sCVD) and poly-crystalline (pCVD) diamonds.

Homoepitaxial sCVD diamonds are grown on high-temperature, high-pressure synthetic diamonds and are therefore restricted in size to about 5 x 5 mm<sup>2</sup>.

For pCVD material, diamond nano-crystals

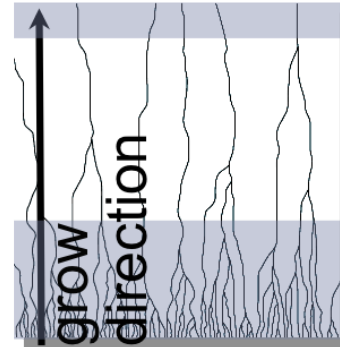


**Figure 1:** Schematics of crystal growth for pCVD diamond material. The number of grain boundaries reduces significantly with the material thickness. The diamond substrate is abraded and polished from both sides to the thickness indicated with white background, which is used as detector material.

which are deposited on a silicon crystal are used as the seed. Due to the non-uniformity of the seed, the grown diamond material consists of randomly oriented crystals which are separated from each other through grain boundaries. These boundaries, which are potential locations for the accumulation of material impurities (such as N, B, Si and others), can act as charge sinks, reducing the charge collection efficiency (CCE) of the material in use and introducing space charge effects. Only through the growth of a very thick substrate, where the top layer is used as detector material, see white area in Figure 1, these effects can be significantly reduced.

In recent years there have been efforts to grow heteroepitaxial diamonds for large-area detector applications, which have comparable material properties to homoepitaxial sCVD diamond. In December 2011 it was reported [4] that diamond substrates, grown on large area iridium crystals (DOI), have a CCE of up to 96% and an energy resolution  $\delta E/E$  of 1.5%, which is already close to the values for sCVD diamond [5].

### 3. The n\_TOF experiment at CERN

The n\_TOF facility was constructed for dedicated cross-section measurements of neutron induced reactions. A Pb spallation target which is impinged by a pulsed proton beam of 20 GeV/c, is used as neutron source. The experimental area, where the measurements take place, is located 185 m downstream from the target. The layout of the facility at CERN can be seen in Figure 2.

A sweeping magnet, positioned after a first collimator for the neutron beam, ensures that charged particles from the spallation process are removed from the neutron beam. The photon background, caused by the spallation process and the subsequent thermalization of the

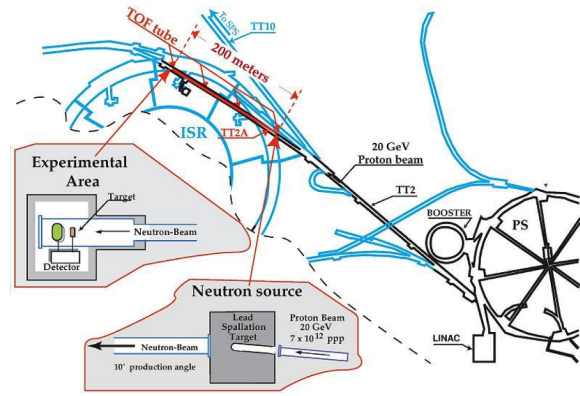


Figure 2: Layout of the n\_TOF facility at CERN.

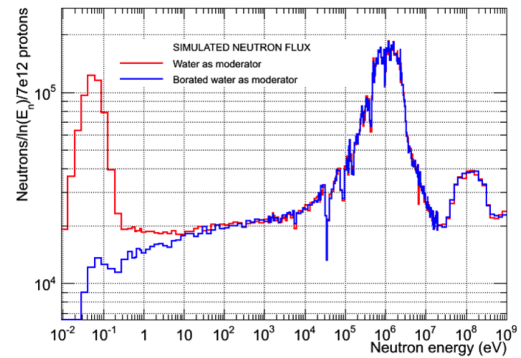


Figure 3: Neutron fluence at n\_TOF, for a collimator of 1.8 cm diameter.

neutrons, remains within the neutron beam. Directly before the experimental area a second collimator is positioned, the inner diameter of which can be adjusted according to the experimental requirements.

The characteristics of the facility are the high instantaneous neutron flux over a wide energy range from thermal up to GeV, see Figure 3, with the neutron energy being determined experimentally via the time-of-flight technique. The long flight path and the narrow proton beam pulse width of 6 ns rms provide an energy resolution of the order of  $10^{-3}$  in the energy region of astrophysical interest.

#### 4. $^{10}\text{B}(n, \alpha)^7\text{Li}$ test measurement

The experimental program at n\_TOF has recently been extended from capture and fission cross-section measurements to the investigation of neutron-induced charged particle (cp) reactions. A critical parameter for the measurement of  $(n, \text{cp})$  reactions is the thickness of the sample containing the isotope of interest, as the produced particles should have only a minor energy loss before escaping the sample. This implies small mass samples. In order to have acceptable statistics during a given measurement, the solid angle covered by the detector should be maximized. This can be achieved by placing the detector directly in the neutron beam. Hence the detector in use for  $(n, \text{cp})$  cross-section measurements should, in addition to having an adequate size to cover the neutron beam, combine a high particle detection efficiency with a low neutron-induced background.

CVD diamond has proven to have a charged particle detection efficiency close to 100% [6]. The  $(n, \alpha)$  reaction on  $^{12}\text{C}$ , being the first significant background reaction channel to open, has a threshold energy of 6.2 MeV and the high radiation tolerance of this material allows the positioning of the detector in the neutron beam. For this measurement sCVD diamonds would have been preferred for their good spectroscopic properties, but only pCVD diamond substrates were available in adequate sizes in order to cover the n\_TOF neutron beam with a full width at half maximum (FWHM) of 2 cm, when using the collimator of 1.8 cm in diameter.

To validate the functionality of the detector setup, the well known  $^{10}\text{B}(n, \alpha)^7\text{Li}$  reaction, standard up to 1 MeV [7], has been chosen for a first measurement.

The objectives of the test measurement were the following:

- To determine the detection efficiency of the pCVD diamond detector for the  $(n, \alpha)$  reaction.
- To investigate the background level of the CVD diamond in the region of interest.
- To identify aspects to be improved for a future CVD diamond detector.

#### 4.1 Prototype detector and experimental setup

For the prototype detector a pCVD diamond of  $20 \times 20 \times 0.5 \text{ mm}^3$  was used [8]. The raw pCVD material showed graphite inclusions, which locally alter the material properties of the diamond.

The diamond was metallized with 100 nm thick, segmented Al electrodes in collaboration with CEA Saclay [9], implementing a 4-pad detector.

The diamond was mounted on a printed circuit board sandwich-structure. The electrical contacts to the 4 pads and the ground electrode were achieved by mechanical clamping. Pad 1 and 3 were biased with -400 V, pad 2 and 4 with -396 V. This introduced a transversal field between adjacent electrodes to minimize field-free regions in the diamond detector.

The signals of each pad were read out on the high voltage (HV) side and amplified with fast, low-noise charge amplifiers [10].

The whole assembly was positioned in the neutron beam. The  $^{10}\text{B}_4\text{C}$  sample was mounted in front of the diamond detector, leaving an air gap of 1 mm to the detector. This gave a solid angle coverage close to 50%.

#### 4.2 Auxiliary measurements

The  $^{10}\text{B}_4\text{C}$  sample was characterized at the Centro Nacional de Aceleradores (CNA) in Sevilla/Spain through Rutherford back-scattering (RBS), which gave a thickness of

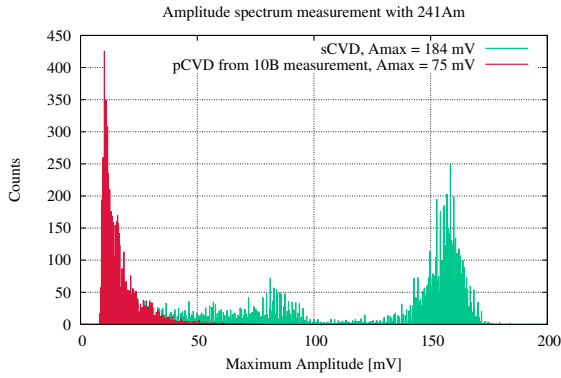


**Figure 4:** Amplitude spectrum of the pCVD detector (red) during the calibration with the  $^{241}\text{Am}$  source. For qualitative comparison the spectrum of a sCVD diamond detector is shown (green).

$1.08 \cdot 10^{-5} \text{ }^{10}\text{B}$  atoms/barn [12].

The geometrical efficiency and the effect of the sample thickness on the outgoing  $\alpha$  particles was simulated using the FLUKA Monte-Carlo code. This simulation showed that 32.7% of all produced  $\alpha$  particles enter the diamond detector with a minimum energy of 500 keV. This energy has been chosen as the lower limit for discrimination of the  $\alpha$  particles from the in-beam  $\gamma$ -background at n\_TOF, which has a comparable energy.

The neutron fluence was monitored via an Au-foil activation, resulting in  $BIF = 0.89$  [11]. The 11% losses of the available neutrons are related to the smaller size of the detector compared to the beam size.

The diamond detector has been calibrated using a  $^{241}\text{Am}$   $\alpha$ -source and a  $^{90}\text{Sr}$   $\beta$ -source. The amplitude spectrum from the calibration with  $^{241}\text{Am}$  can be seen in Figure 4 in comparison to a sCVD diamond detector. The spectrum recorded with the sCVD diamond shows the  $\alpha$  peak around 155 mV. As expected, the pCVD diamond exhibits less amplitude, due to the reduced CCE of about 40% [8]. Its spectrum does not show the alpha peak, which demon-

strates insufficient spectroscopical properties. With the trigger set to 6 mV, the mean value of the amplitude spectrum of the pCVD diamond detector is 16.8 mV and the standard deviation 8.2 mV, which gives an energy resolution of 49%. Upon calibration with a  $^{90}\text{Sr}$  source the counting rate was of comparable magnitude for both materials.

### 4.3 Experimental data

The amplitude spectra of the  $\alpha$  particles produced via the  $^{10}\text{B}(n, \alpha)$  reaction and the recorded background have been compared for each of the 4 pads (DIAM1-4). An amplitude threshold for the experimental data was set for each of the detector pads, taking the different gains of the preamplifiers into account, dismissing noise events, and rejecting part of the background.

During the experimental campaign, to record the background, a measurement without the  $^{10}\text{B}$  sample was performed. The background spectra as a function of neutron energy can be seen in Figure 5, for each of the detector pads.

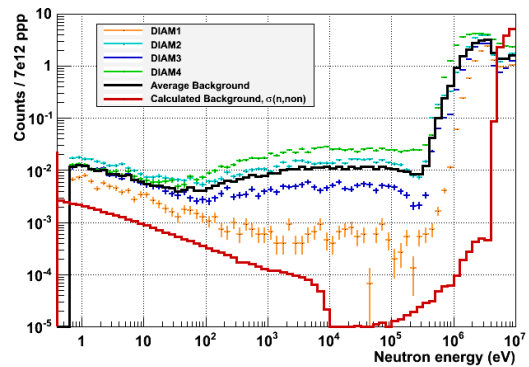


**Figure 5:** Recorded background for all 4 detector pads (DIAM1-4) as a function of neutron energy. The averaged background is shown in black. The red curve corresponds to the theoretical background, taking the thickness of the diamond detector and all the non-elastic neutron-induced reactions on  $^{12}\text{C}$  into account.



The contribution of the n\_TOF specific in-beam  $\gamma$ -background can be seen in the energy region from 100 eV to a few hundred keV. The difference between the pads is related to their relative position in the Gaussian neutron beam profile.

The elastic scattering of neutrons on  $^{12}\text{C}$ , which is present throughout the neutron spectrum, is visible at neutron energies above 300 keV.

At low energies, where the spectrum follows a  $1/E$  characteristic, the experimental data is 10 times higher than expected, see Figure 5. This can be explained by either B or N impurities in the diamond material. B would contribute through the  $(n, \alpha)$  and N through the  $(n, p)$  reaction.

The experimental spectrum recorded during

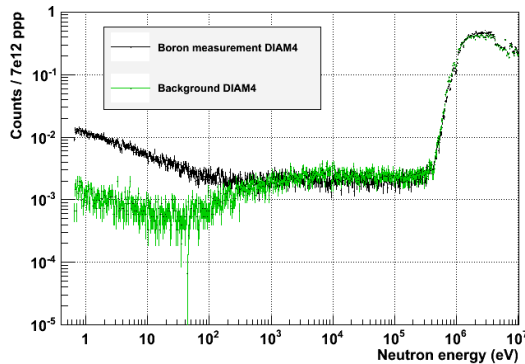


**Figure 6:** Experimental spectrum for the detector DIAM4. The measured  $^{10}\text{B}$  spectrum is plotted in black. The spectrum recorded during the background measurement is shown in green.

the  $^{10}\text{B}$  measurement in comparison with the background spectrum for one of the detector pads can be seen in Figure 6. The background from in-beam  $\gamma$ -rays dominates for  $E_n \geq 100$  eV. With a better energy resolution of the detector material it would be possible to reduce the background significantly, as a classification of the measured particles would be possible through the amplitude spectrum.

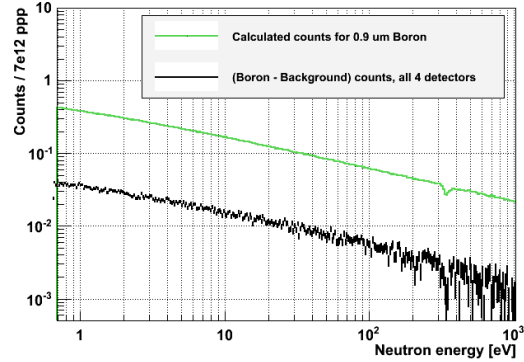


**Figure 7:** Recorded  $^{10}\text{B}(n, \alpha)^7\text{Li}$  events in total (black) for neutron energies up to 1 keV. For the calculated, expected spectrum (green), the neutron fluence, sample thickness and efficiency are taken from the auxiliary measurements (see text for details). The ratio of the two graphs shows that about 9% of the expected  $^{10}\text{B}(n, \alpha)^7\text{Li}$  events could be distinguished with the prototype detector.

#### 4.4 Results

The experimental result for each of the detectors is calculated as the difference between the recorded  $^{10}\text{B}$  and the background spectrum, corresponding to  $C(E_n) - B(E_n)$  in equation (1.2).

In Figure 7 the result of the measurement is plotted in comparison with the expected result, normalized to pulses of  $7 \cdot 10^{12}$  protons on target. The green graph in Figure 7 includes the results of the auxiliary measurements for the neutron fluence, the sample thickness and the efficiency of the detector setup.

9% of the expected counting rate was actually measured, giving an overall efficiency  $\varepsilon = 3\%$ .

## 5. Conclusion

The results of a measurement of the  $^{10}\text{B}(n, \alpha)^7\text{Li}$  reaction with a prototype detector based on the CVD diamond technology were presented.

The overall efficiency of the measurement was  $\varepsilon = 3\%$  instead of the expected 50%, which are a consequence of the  $2\pi$  geometry of the experimental setup. This discrepancy can be explained by the insufficient energy resolution of 49% for the detector material in use, which inhibited the rejection of a significant part of the recorded background, caused by both in-beam  $\gamma$  and elastic scattering of neutrons on  $^{12}\text{C}$ . A classification of particles through the amplitude spectrum of the experimental data was not possible.

For future applications of CVD diamonds in the field of  $(n, \text{cp})$  cross-section measurements, the following points need to be implemented:

- The detector material needs to have an energy resolution comparable to sCVD diamond material, so that background events can be identified in the amplitude spectrum and dismissed from the spectrum.
- The impurities in the diamond material should be as few as possible, in order to reduce neutron-induced background.
- The detector material should not have defects like graphite inclusions, in order to have homogeneous material properties throughout the detector.
- For additional background minimization, the thickness of the diamond should be reduced.
- The size of the detector should be enlarged in order to cover more of the available neutron beam.
- The whole assembly should be placed in vacuum, to minimize the energy loss of the produced particles on their way to the detector.
- To implement a geometry close to  $2*2\pi$ , a sample should be positioned on either side of the detector.

For the near future, a measurement that should fulfill all these requirements has been already proposed at CERN [13]. The  $^{59}\text{Ni}(n, \alpha)^{56}\text{Fe}$  cross-section with a large area, 250  $\mu\text{m}$  thick DOI diamond [4] will be measured.

## References

- [1] C. Rubbia et al., *A high Resolution Spallation driven Facility at the CERN-PS to measure Neutron Cross Sections in the Interval from 1 eV to 250 MeV*, CERN/LHC/98-02 (EET), (1998); CERN/LHC/98-02 (EET)-Add.1, (1998).
- [2] H. Fraiss-Koelbl et al., *A Fast Low-Noise Charged-Particle CVD Diamond Detector*, IEEE Transactions on Nuclear Science, Vol.51, No. 6 (2004).
- [3] H. Pernegger et al., *Charge-carrier properties in synthetic single-crystal diamond using the transient-current Technique* J.Appl.Phys. 97, 073704 (2005).
- [4] <http://www-carat.gsi.de/>.
- [5] E. Griesmayer et al., *High-Resolution Energy and Intensity Measurements with CVD Diamond at REX-ISOLDE*, CERN BE-Note-2009-028 (2009).
- [6] M. Rebisz et al., *CVD diamond dosimeters for heavy ion beams*, Diam.&Rel.Mat. 16, 1070-1073 (2007).
- [7] A. D. Carlson et al., *International Evaluation of Neutron Cross Section Standards*, Nuclear Data Sheets 110, 3215-3324 (2009).
- [8] Diamond Detectors Ltd., <http://www.diamonddetectors.com/>.

- [9] P. Bergonzo, M. Pomorski, LIST CEA Saclay.
- [10] CIVIDEC Instrumentation GmbH, [www.cividec.at](http://www.cividec.at).
- [11] N. Sabbi, Private communication, June 2011.
- [12] J. Praena, Private communication, October 2011.
- [13] C. Weiss et al., *The  $(n, \alpha)$  reaction in the  $s$ -process branching point  $^{59}\text{Ni}$*  CERN-INTC-2012-011, INTC-P-327.